Available online at www.sciencedirect.com

SciVerse ScienceDirect

journal homepage: www.elsevier.com/locate/he

Sorption behavior of the MgH_2–Mg_2FeH_6 hydride storage system synthesized by mechanical milling followed by sintering

Julián Puszkiel [a,b,*], Fabiana Gennari [a], Pierre Arneodo Larochette [a], Fahim Karimi [b], Claudio Pistidda [b], Rapee Gosalawit-Utke [b,c], Julian Jepsen [b], Torben R. Jensen [d], Carsten Gundlach [e], José Bellosta von Colbe [b], Thomas Klassen [b], Martin Dornheim [b]

[a] Instituto Balseiro (UNCuyo and CNEA), Consejo Nacional de Investigaciones Científicas y Técnicas (CONICET) and Centro Atómico Bariloche, Av. Bustillo km 9.5, S. C. de Bariloche R8402AGP, Argentina
[b] Institute of Materials Research, Materials Technology, Helmholtz-Zentrum Geesthacht, Geesthacht 21502, Germany
[c] School of Chemistry, Institute of Science, Suranaree University of Technology, Nakhon Ratchasima 30000, Thailand
[d] Center for Energy Materials, iNANO and Department of Chemistry, University of Aarhus, Aarhus C8000, Denmark
[e] MAX-lab, Lund University, Lund S-22100, Sweden

ARTICLE INFO

Article history:
Received 25 May 2013
Received in revised form
6 August 2013
Accepted 16 August 2013
Available online 1 October 2013

Keywords:
Hydride mixture
Magnesium hydride
Complex hydride
Reaction path
Desorption kinetics

ABSTRACT

The hydrogen sorption behavior of the Mg_2FeH_6–MgH_2 hydride system is investigated via in-situ synchrotron and laboratory powder X-ray diffraction (SR-PXD), differential scanning calorimetry (DSC), scanning electron microscopy (SEM), particle size distribution (PSD) and volumetric techniques. The Mg_2FeH_6–MgH_2 hydride system is obtained by mechanical milling in argon atmosphere followed by sintering at high temperature and hydrogen pressure. In-situ SR-PXD results show that upon hydriding MgH_2 is a precursor for Mg_2FeH_6 formation and remained as hydrided phase in the obtained material. Diffusion constraints preclude the further formation of Mg_2FeH_6. Upon dehydriding, our results suggest that MgH_2 and Mg_2FeH_6 decompose independently in a narrow temperature range between 275 and 300 °C. Moreover, the decomposition behavior of both hydrides in the Mg_2FeH_6–MgH_2 hydride mixture is influenced by each other via dual synergetic-destabilizing effects. The final hydriding/dehydriding products and therefore the kinetic behavior of the Mg_2FeH_6–MgH_2 hydride system exhibits a strong dependence on the temperature and pressure conditions.

* *Corresponding author*. Instituto Balseiro (UNCuyo and CNEA), Consejo Nacional de Investigaciones Científicas y Técnicas (CONICET) and Centro Atómico Bariloche, Av. Bustillo km 9.5, S. C. de Bariloche R8402AGP, Argentina.
E-mail address: jpuszkiel@cab.cnea.gov.ar (J. Puszkiel).
0360-3199/$ – see front matter
http://dx.doi.org/10.1016/j.ijhydene.2013.08.068

1. Introduction

Due to the highest known volumetric hydrogen density (150 kg H_2 m^{-3}) and a gravimetric hydrogen density of 5.4 wt.%, Mg_2FeH_6 is considered a promising material for hydrogen storage. It is also an interesting material for energy storage owing to its high dissociation enthalpy of about 90 kJ/mol H_2 [1–5]. Moreover, Mg and Fe are low cost and abundant metals. However, because of the absence of a Mg_2Fe intermetallic compound [6], pure Mg_2FeH_6 is difficult to synthesize. Several attempts were done to prepare pure Mg_2FeH_6 from 2Mg–Fe and $2MgH_2$–Fe stoichiometric mixtures. Methods such as thermal treatment like sintering or hydrogen cycling [1,2,7–9], mechanical milling (MM) in argon and hydrogen atmosphere [10–22] and combinations of the methods mentioned before were utilized [3,23–25]. Most of these methods involved extreme temperature and pressure conditions: 450–500 °C and 1.5–12 MPa for the sintering process, MM for 60–270 h or more than 20 hydrogen absorption–desorption cycles. Despite these conditions, pure Mg_2FeH_6 was hardly obtained. Thus, the Mg_2FeH_6–MgH_2 mixture is commonly the reversible hydride system.

The formation mechanism of Mg_2FeH_6 via MM in hydrogen and heating under hydrogen was also investigated [2,11,26–28]. Bodanovič et al. [2] proposed different reaction paths based on equilibrium measurements from 2:1, 4:1 and 1:1 Mg:Fe stoichiometric mixtures. From 2:1 and 1:1 Mg–Fe mixtures, Bodanovič et al. suggested the formation of Mg_2FeH_6 from 2Mg, Fe and H_2. Moreover, from a 4Mg:Fe mixture, the formation of Mg_2FeH_6–MgH_2 was also proposed. Hauback et al. [26] also obtained the direct synthesis of Mg_2FeH_6 from 2Mg, Fe and H_2 at 349 °C and low pressure (0.49 MPa) starting from an as-milled 2Mg–Fe material. On the contrary, Polanski et al. [27] showed through in-situ synchrotron X-ray diffraction measurements that MgH_2 is a precursor for the Mg_2FeH_6 formation in dynamic conditions, following a two-step reaction, i.e. first MgH_2 and then Mg_2FeH_6 formation. Gennari et al. [11] first observed that the synthesis of Mg_2FeH_6 from 2Mg:Fe via MM in hydrogen atmosphere occurred through MgH_2 as an intermediate phase following a two-step simultaneous reaction mechanism, i.e. the MgH_2 and Mg_2FeH_6 formation at the same time. Finally, Zhang et al. [28] confirmed the two-step simultaneous reaction mechanism milling a 2Mg–Fe stoichiometric mixture in hydrogen. The hitherto results proved that the reaction paths to obtain the Mg_2FeH_6 are highly influenced by the microstructural characteristics of the material, procedure (MM or heating) and pressure–temperature conditions. Regarding the desorption behavior, Polanski et al. showed that Mg_2FeH_6 decomposes into Mg, Fe and H_2 [27].

It is well known that Fe has a catalytic effect during the MgH_2 formation/decomposition on the dissociation/recombination of the hydrogen molecule, respectively [29,30]. In many works the hydrogen sorption properties of MgH_2 catalyzed by Fe were investigated [31–35]. In others, the hydrogen sorption properties of Mg_2FeH_6–MgH_2 were studied [3–5,12,15–17,19,21,22]. It was found that above 375 °C the hydrogen absorption rate slows down because of the Mg_2FeH_6 formation [5]. The desorption kinetic behavior of the Mg_2FeH_6–MgH_2 mixture was analyzed via thermal analysis [12,15–17,21,22]. Zhou et al. concluded that Mg_2FeH_6 can reduce the structural stability of MgH_2 and further improve its dehydrogenation properties [17].

In spite of all the published results, many aspects of the Mg_2FeH_6–MgH_2 mixture such as its in-situ formation/decomposition, the influence of temperature and pressure upon its formation and desorption kinetics was not exhaustively investigated.

In this work, the Mg_2FeH_6–MgH_2 hydride system is investigated via several techniques. The reaction paths of the Mg–Fe–H system upon hydriding and dehydriding are studied by in-situ SR-PXD (Synchrotron Radiation – Powder X-ray Diffraction). Volumetric techniques as well as calorimetric (DSC – Differential Scanning Calorimetry) measurements are utilized to examine the Mg–Fe–H system sorption behavior in dynamic conditions. Additional characterization techniques such as laboratory PXD, SEM (Scanning Electron Microscopy) and PSD (Particle Size Distribution) are also performed to understand the Mg–Fe–H system reaction paths and sorption behaviors.

2. Experimental

The investigated hydride system was synthesized via 100 h of mechanical milling in argon atmosphere followed by sintering as explained in references [4,5]. Additional experiments were carried out with a $2MgH_2$ + Fe stoichiometric mixture (MgH_2 > 99.99%, Sigma Aldrich and Fe > 99.5%, Riedel – de Haën) milled for 2 h and sintered several times at 450 °C and 6.0 MPa of H_2 for 24 h. In-situ synchrotron radiation powder X-ray diffraction (SR-PXD), laboratory PXD (Lab PXD), differential scanning calorimetry (DSC), scanning electron microscopy (SEM), particle size distribution (PSD) and volumetric (Sieverts devices) techniques were used to investigate the characteristic properties of the obtained Mg_2FeH_6–MgH_2 hydride mixture [36–39].

The absorption and desorption reaction paths under dynamics and non-isothermal conditions were studied via in-situ SR-PXD. The in-situ SR-PXD measurements were carried out in the MAX II Synchrotron in Lund, Sweden, at Beamline I711 in the research laboratory MAXlab using a X-ray wavelength of $\lambda = 0.99917$ Å and a Mar 165 CCD detector for data collection [36]. The samples (0.5–2 mg) were airtight encapsulated in a sapphire capillary and then mounted in a specially developed sample holder [37]. The sample holder was connected to the gas system, which was filled with argon and evacuated till vacuum three times before opening the valve to the sample and starting the experiment. For the hydriding in-situ SR-PXD, a 2Mg–Fe stoichiometric mixture after the preparation process (100 h of MM in Ar followed by sintering and subsequent dehydrogenation at 400 °C and 20 kPa) was hydrided at 5.0 MPa of H_2 from RT to 400 °C with isothermal processes at 300, 350 and 400 °C. For the dehydriding in-situ SR-PXD, a 2Mg–Fe stoichiometric mixture after the preparation process (100 h of MM in Ar followed by sintering) was dehydrided at 0.1 MPa of H_2 from RT to 400 °C. For both hydriding and dehydriding processes a constant heating rate of 3 °C/min was used. In order to study the formation/

decomposition of the MgH_2 and Mg_2FeH_6 hydride phases, the peak areas were calculated and showed as a function of temperature or time.

Lab PXD (Philips PW 1710/01 Instruments, CuK_a radiation, $\lambda = 1.5405$ Å, graphite monochromator, 30 mA and 40 kV) was performed to characterize the crystalline phase in the samples after hydrogen interaction at different temperature and pressure conditions. The crystallite size was calculated by the Scherrer equation [40]. The thermal behavior of the samples under argon atmosphere was studied by DSC (DSC, TA Instruments 2910 calorimeter) using different heating rates of 1, 2, 5, 10, 15 and 25 °C min^{-1} and argon flow rate of 122 ml min^{-1}. From the DSC curves, the activation energy (E_a) of the desorption process was calculated by the Kissinger method [41]. Morphological analyses of powder samples dispersed on a stick were performed by scanning electron microscopy (SEM 515, Philips Electronic Instruments). Moreover, the agglomerate size distributions of the as-milled 2Mg–Fe powder material was determined by using Mastersizer Micro MAF 5000 device which range of measurement lay between 0.3 and 300 μm. The sample was diluted in N-butane and stirred at 2100 rpm and then the measurement was performed. The volumetric technique (Sieverts devices [38,39]) was utilized to investigate the temperature and pressure effects upon the Mg_2FeH_6–MgH_2 hydride mixture in dynamic conditions and the mechanisms related to the absorption process. The hydrogen absorption rates were measured using the Sieverts method, while the hydrogen desorption rates were measured through a mass flow controller in a Sieverts type apparatus [38]. In order to examine only the temperature effect upon the hydride mixture, we performed measurements at 350, 375 and 400 °C and constant relationship between the initial absorption pressure and the equilibrium pressure of the Mg_2FeH_6–MgH_2 hydride mixture at each temperature ($P_i/P_{eq.} = 2.7$; the equilibrium pressures of the Mg_2FeH_6–MgH_2 hydride mixture are reported in Refs. [4,5]). To study the pressure effects, measurements at different relationship between the initial absorption pressure and the equilibrium pressure of the Mg_2FeH_6–MgH_2 hydride mixture were done at 300 °C (range of initial pressures of the system: 0.6–4.3 MPa), at 350 °C (range of initial pressures of the system: 0.9–4.4 MPa) and at 450 °C (range of initial pressures of the system: 2.1–4.4 MPa). To assess the temperature and pressure effects on the Mg_2FeH_6–MgH_2 hydride mixture, the synthesized material was dehydrided and then rehydrided at the above mentioned conditions. All the absorption curves are reported as hydrogen fraction vs. time (hydrogen fraction: ratio between the hydrogen capacity absorbed during the measurement and the saturation capacity of the material). In order to study the absorption mechanism during hydriding, a sintering process was carried out from as-milled 2Mg–Fe at 400 °C and 12 MPa in the Sieverts device: HERA Hydrogen Systems, Quebec, Canada [39]. The hydrogen desorption rates were measured through a mass flow controller at 300, 350 and 400 °C and from a pressure above the desorption equilibrium pressure of the Mg–Fe–H system down to vacuum pressure (20 kPa). It is important to mention that the flow mass controller can take out smaller amounts of hydrogen than those released from the sample, mainly at 350 and 400 °C. Thus, the hydrogen release is limited by the flow mass controller capacity. For this reason, the desorption rate curves are only useful to identify the hydride phase(s) in the material. To carry out each measurement roughly 100 mg of material was used in order to minimize the heat and mass transfer problems through the powder bed [30].

All handling was carried out in MBraun Unilab globe boxes with oxygen and moisture controlled argon atmosphere (concentrations of <5 ppm of O_2 and H_2O), so as to prevent the oxidation of the samples.

3. Results and discussion

3.1. Reaction paths of the Mg–Fe–H hydride system

3.1.1. Hydrogenation path of the Mg–Fe–H hydride system

In our previous works [4,5], the hydrogen storage properties of the Mg–Fe–H hydride system, synthesized by MM (100 h in Ar) of 2Mg–Fe powder blends and subsequent sintering (400 °C and 6.0 MPa for 15 h) were investigated. Herein, in order to gain a deeper understanding of the studied Mg–Fe–H hydride system, the same as-milled and sintered 2Mg–Fe material was utilized [4]. The stored capacity of the sintered 2Mg–Fe was about 4.5 wt.%. The phases detected by PXD (not shown) after sintering were Mg_2FeH_6, MgH_2 and unreacted Fe. The relative amounts of MgH_2 and Mg_2FeH_6 were about 20 wt.% and 50 wt.%, respectively [4,5]. After sintering, the Mg_2FeH_6 and MgH_2 hydride phases had crystallite sizes of 30 and 40 nm, respectively, while the unreacted Fe had a crystallite size of 30 nm as well as in the as-milled sample. After Mg_2FeH_6 and MgH_2 decomposition, the crystallite sizes for Mg and Fe were 30 nm. Additionally, the as-milled 2Mg–Fe material was also sintered at 400 °C and 12.0 MPa for 15 h in a HERA Hydrogen Systems Sieverts device [39]. The obtained capacity, phases and microstructure were similar to the material sintered at 6.0 MPa. Thus, the pressure did not caused any effect in the yield of Mg_2FeH_6. Moreover, a fitting of gas–solid reaction integral models [42] to the absorption curves corresponding to sintering for both pressures (6.0 and 12 MPa – curves and fitting not shown) suggested that the reaction is controlled by 3D – diffusion mechanisms. Therefore, in order to investigate the absorption path and mechanisms of the Mg–Fe–H system several characterizations and experiments were performed.

Fig. 1 shows sticker-mounted SEM micrographs of the as-milled (Fig. 1A and B) and sintered (Fig. 1C and D) 2Mg–Fe samples. As seen in Fig. 1A and C, the 2Mg–Fe agglomerate sizes are between 50 and 300 μm. This agglomerate size distribution is in agreement with the obtained from PSD analysis of the as-milled 2Mg–Fe sample which is between 100 and >300 μm (average volume agglomerate size: 200 μm). Thus, the agglomerate size distributions of the as-milled and sintered samples are practically alike with an average value of 200 μm. For both samples (Fig. 1B and D) the surface is rather compact. However, the sintered sample shows some cracks on the surface and small agglomerates with irregular shapes owing to the sintering process.

In-situ SR-PXD [36] analysis of the hydriding process of a 2Mg–Fe stoichiometric mixture was carried out (as-milled and sintered 2Mg–Fe sample desorbed at 400 °C and 20 kPa in a Sieverts kind device [38]) (Fig. 2). The measurement was

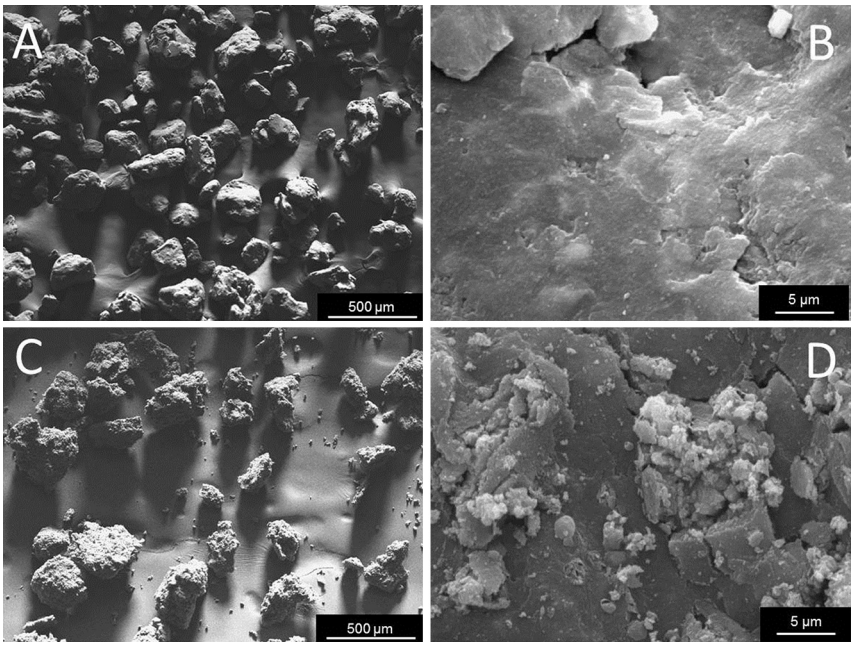

Fig. 1 – Secondary electron SEM micrographs of stick mounted samples: A and B – As-milled 2Mg–Fe stoichiometric mixture. C and D – Milled and sintered 2Mg–Fe stoichiometric mixture.

performed at 5.0 MPa from 30 to 400 °C with a heating rate of 3 °C/min, dwelled at 300, 350 and 400 °C for about 25 min Fig. 2A shows the entire hydriding process from which the formation of first MgH_2 and second Mg_2FeH_6 can be noticed. In Fig. 3, the peak areas calculated using the in-situ SR-PXD (Fig. 2) in the same range of temperatures from 200 up to 250 °C (Fig. 3A), during the isothermal periods at 350 °C (Fig. 3B) and 400 °C (Fig. 3C) can be observed. From 215 to 240 °C, MgH_2 is formed and metallic Mg is totally consumed (Figs. 2A and 3A). Then, between 240 and 350 °C, MgH_2 is still the unique hydride phase (Fig. 2A). Mg_2FeH_6 appears during the isothermal process at 350 °C (Figs. 2B and 3B). As seen in Fig. 3B, the peak area of Mg_2FeH_6 starts to increase after about 7 min, while the peak areas corresponding to MgH_2 and Fe tend to decrease. During the constant temperature process at 400 °C, the same tendency observed at 350 °C steadily continues (Fig. 3C). Finally, at the end of the thermal process, Mg_2FeH_6, MgH_2 and remnant Fe are observed (Fig. 2A). This result provides a clear insight of the hydriding path of the Mg–Fe–H system under dynamic conditions. Hence, it can be concluded that MgH_2 is a precursor for the Mg_2FeH_6 formation. Polanski et al. [27] also observed the formation of Mg_2FeH_6 from MgH_2 by SR-PXD (hydriding a 2Mg–Fe sample at 10 MPa). On the other hand, Hauback et al. [26] obtained Mg_2FeH_6 from the direct hydrogenation of Mg and Fe at 349 °C and 0.49 MPa for about 20 h. This fact is attributed to the different absorption equilibrium pressures of the Mg_2FeH_6 (0.36 MPa [2]) and MgH_2 (0.57 MPa [43]) hydride phases. Furthermore, the direct formation of Mg_2FeH_6 at the above mentioned mild conditions was rather slow (20 h) suggesting strong kinetic constraints, i.e. diffusion constraints. At 349 °C and high hydrogen pressure of 2.8 MPa, the absorption rate was much faster and the obtained amount of Mg_2FeH_6 was reduced by the simultaneous formation of MgH_2 [26]. Hence, this result implies that at relative low temperature and high pressure, the MgH_2 formation is kinetically favored.

In our case, the Mg_2FeH_6–MgH_2 hydride mixture just exhibits one absorption equilibrium pressure [4,5]. This fact can be related to the following characteristics: (1) according to the literature [2,43], the absorption equilibrium pressure of MgH_2 is only slightly higher than that corresponding to Mg_2FeH_6; (2) the apparent equilibrium pressure of MgH_2 is strongly affected by the initial state of Mg as for examples particle size distribution [44] and the related reaction kinetics; (3) as Mg and Fe have a positive enthalpy of mixing and hydrogen diffusion is much faster than Fe diffusion, the direct formation of Mg_2FeH_6 from Mg and Fe even in equilibrium conditions might not be favored leading first to the MgH_2 formation. Thus, the described characteristics may not allow to measure two equilibrium pressures for the Mg–Fe–H under the given experimental conditions. During the experiment, though, a pressure of 5.0 MPa of hydrogen was used. Hence, it is possible to neglect any influence of the driving force upon the absorption behavior of the Mg–Fe–H hydride system ($P_{experiment}/Peq_{400\ °C} = 2.8$). Additionally, based on the results shown in Figs. 2 and 3, a competitive effect between the Mg_2FeH_6 and MgH_2 formation is also discarded. Now, the following questions arise: (1) – Why just MgH_2 is formed at 215 °C?, (2) – Why does Mg_2FeH_6 appears after about 7 min at 350 °C? and (3) – What does preclude the Mg_2FeH_6 further formation from MgH_2?

The 2Mg–Fe material in equilibrium and dynamic conditions at temperatures lower than 350 °C reacts with hydrogen towards the formation of MgH_2 catalyzed by Fe [4,5]. Hence, at low temperatures the common atom diffusion mechanism that involves the Mg_2FeH_6 formation is hindered. Once MgH_2 is formed at 350 °C after a while the reaction with Fe to form Mg_2FeH_6 is observed. Considering the diffusion coefficient of hydrogen in

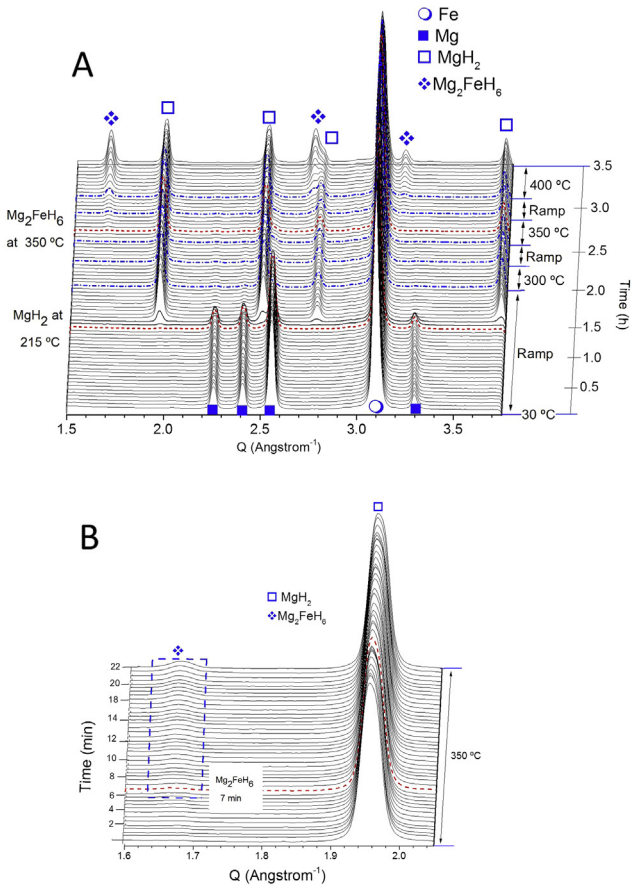

Fig. 2 – In-situ SR-PXD of a 2Mg–Fe stoichiometric mixture after the preparation process. A – Hydriding from 30 to 400 °C with isothermal processes at 300, 350 and 400 °C and 5.0 MPa of H_2. B – Zoom of the hydriding process during the isothermal condition at 350 °C and 5.0 MPa. Heating rate ~ 3 °C/min.

MgH_2 calculated for a powder of an average diameter of 100 μm between 300 and 400 °C [45], an estimation of the mean diffusion time ($t_{mean} = d^2/6D$; d: particle diameter, D: diffusion coefficient) for $d \sim 200$ μm and $D_{350°C} \sim 1.06 \times 10^{-7}$ cm^2/s leads to a t_{mean} of about 10 min at 350 °C. This result agrees very well with the average agglomerate size observed by SEM (Fig. 1) and measured by PSD analysis and the time at which the Mg_2FeH_6 is detected by the SR-PXD during the dwelling at 350 °C (Figs. 2B and 3B). Based on this analysis, it is possible to assume that MgH_2 can act as a hydrogen diffusion barrier for the initial formation of Mg_2FeH_6 [46]. Hauback et al. suggested the same diffusion mechanism for materials obtained by cryomilling and hydrided at 349 °C and different hydrogen pressures [26]. According to previous works [2,27], Mg_2FeH_6 formation takes place at the phase boundary between Fe seeds and the growing hydride phase. Therefore, once a thick layer of Mg_2FeH_6 is formed between MgH_2 and Fe, the reaction between the outer MgH_2 and the Fe seeds can be precluded by solid–solid diffusion effects [19,47]. At 400–500 °C, temperatures at which the sintering processes are carried out [1,2,4–9], the diffusion of hydrogen though MgH_2 cannot be the main barrier since the diffusion coefficient increases exponentially with the temperature (t_{mean} in the order of seconds).

In order to further clarify the described hydriding mechanism and to obtain only Mg_2FeH_6 hydride phase, experiments were carried out with a sample composed of $2MgH_2 + Fe$. This sample was milled for two hours in Ar atmosphere and sintered at 450 °C and 6.0 MPa in a muffle for 24 h. This process was repeated four times till obtaining a material composed only of Mg_2FeH_6 plus remnant Fe. In Fig. 4A, the PXD analyses show that MgH_2 is progressively consumed throughout the thermal processes, which can be associated with the effect of the previous mechanical milling, changing the microstructural characteristics of the material. This suggests that during the intermediate milling process the layer of Mg_2FeH_6 as well as MgH_2 and Fe grain/particle sizes are reduced and the material more homogenously mixed, so that MgH_2 and Fe can further react during sintering.

The DSC curves of the desorption processes shown in Fig. 4B correspond to materials with different compositions. After 2 h of milling, the DSC curve (Fig. 4B(a)) only belongs to MgH_2 catalyzed by Fe in a stoichiometric proportion 2:1. Then, for the first, second and third thermal processes the endothermic events (Fig. 4B(b), (c) and (d)) correspond to the Mg_2FeH_6–MgH_2 hydride mixture. Finally, after the fourth thermal process, the endothermic event comes from Mg_2FeH_6 plus remnant Fe (Fig. 4B(e)). Just in the second thermal process, where the material contains higher proportion of MgH_2 than in the subsequent thermal processes, two endothermic events are clearly seen. Considering that the obtained amount of both hydride phases after the sintering are significant

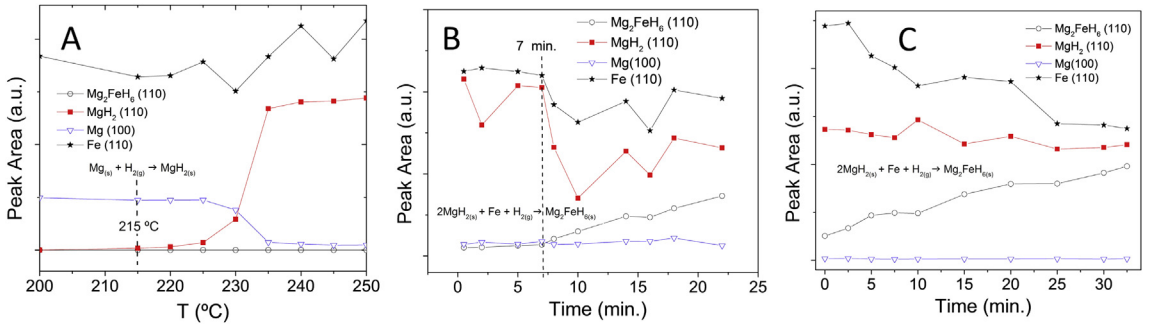

Fig. 3 – Peak areas calculated from the absorption in-situ SR-PXD shown in Fig. 2. A – Peak areas as a function of the temperature from 200 to 250 °C. B – Peak areas as a function of the time at 350 °C. B – Peak areas as a function of the time at 400 °C.

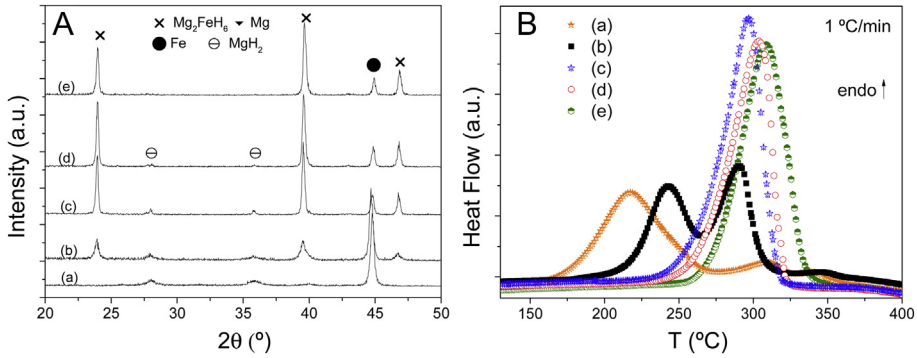

Fig. 4 – A – Lab. PXD and B – DSC of as-milled $2MgH_2$ + Fe at different stages: (a) – milled for 2 h (b) as-milled and then subjected to the first thermal process (450 °C and 6.0 MPa for 24 h in muffle) plus 2 h of MM). (c) as-milled + the second thermal process. (d) as-milled + the third thermal process. (e) as-milled + the third thermal process.

(MgH_2 ~ 20 wt.% and Mg_2FeH_6 ~ 50 wt.% [4,5]), it is expected a similar decomposition behavior as observed in Fig. 4B – curve (b). Now the question arises: What thermal process does the decomposition of Mg_2FeH_6 and MgH_2 account for? These facts lead to the study of the dehydrogenation path in dynamic conditions which will be developed in the following sections.

3.1.2. *Dehydrogenation path of the Mg–Fe–H hydride system*

In order to shed light on the desorption path of the Mg_2FeH_6–MgH_2 hydride mixture, an in-situ SR-PXD was performed. This measurement was carried out with a 2Mg–Fe absorbed sample (milled + sintered sample). The in-situ SR-PXD (Fig. 5) was performed at 0.1 MPa from 30 to 400 °C at a heating rate of 3 °C/min. In Fig. 5A, the entire in-situ SR-PXD is presented and two patterns are highlighted in dash–dot and dash lines at 275 and 285 °C, associated with the beginning of MgH_2 and Mg_2FeH_6 decompositions, respectively.

As clearly seen in Fig. 5B, the peak area of MgH_2 starts to diminish at 275 °C, while that corresponding to Mg begins to increase. From 275 to 285 °C, Mg_2FeH_6 and Fe peak areas remain practically stable. At 295 °C the MgH_2 peak completely disappears. From 285 to about 300 °C, the peak area of Mg_2FeH_6 noticeable decreases and finally disappears. Additionally, the peak area of Fe increases. Taking into account that MgH_2 has higher desorption equilibrium pressure than Mg_2FeH_6, the thermodynamic driving force favors first the MgH_2 decomposition [4,5]. Based on ex-situ PXD and DSC measurements, Gennari et al. [12] reported that a material composed of Mg_2FeH_6 + remnant Fe obtained by milling in H_2 atmosphere decomposes toward Mg and Fe between 260 and 360 °C. Furthermore, Polansky et al. [27] also observed by in-situ SR-PXD that a Mg_2FeH_6 + remnant Fe mixture desorbs hydrogen at about 340 °C giving as products elemental Mg and Fe. In Fig. 5C, the derivatives of the peak areas corresponding to the MgH_2 and Mg_2FeH_6 decompositions as a function of the temperature are shown. It can be noticed that both decomposition processes are overlapped and the peak maxima at 285 and 290 °C correspond to MgH_2 and Mg_2FeH_6, respectively. Hence, these results suggest that MgH_2 and Mg_2FeH_6 decompose independently in a narrow temperature range. First MgH_2 starts to decompose in elemental Mg. Then, overlapped with MgH_2 decomposition, Mg_2FeH_6 decomposes directly in elemental Mg and Fe. The MgH_2–Mg_2FeH_6 hydride mixture decomposition behavior observed by in-situ SR-PXD can be associated with the DSC curve of the first thermal process (Fig. 4B(b)) where two endothermic events are observed. The fact that one endothermic event is noticed for the MgH_2–Mg_2FeH_6 hydride mixture for the second and third thermal processes (Fig. 4B(c) and (d)) might be ascribed to the tiny amounts of MgH_2 and microstructural characteristics of the materials. This last issue is investigated more in detail in the subsequent sections, where the temperature and pressure effects upon in the sorption behavior of the MgH_2–Mg_2FeH_6 hydride mixture are analyzed.

3.2. *Sorption behavior of the Mg_2FeH_6–MgH_2 hydride mixture*

3.2.1. *Temperature and pressure effects*

In Fig. 6, the absorption and desorption curves of the Mg_2FeH_6–MgH_2 hydride mixture at 300, 350 and 400 °C and several pressures are shown. The measurements were carried out as explained in Section 2. The absorption curves (Fig. 6A, C and E) exhibit a clear dependence on the pressure, mainly at 350 and 400 °C. At lower driving forces, nearby the absorption equilibrium pressure of the Mg_2FeH_6–MgH_2 hydride mixture, the absorption rates are slow. The desorption curves (Fig. 6B, D and F) correspond to the shown absorption rates (Fig. 6A, C and E). As seen in Fig. 6B, D and F, the desorption processes evolve into one or two steps. In the case of a two step process (Fig. 6D(1), F(1) and (4)), this fact is related to the desorption equilibrium pressures of Mg_2FeH_6–MgH_2 hydride mixture and the used method to carry out the measurement. In previous works [4,5], it was found that MgH_2 has a higher desorption equilibrium pressure than Mg_2FeH_6. Additionally, the desorption measurements are performed from an initial pressure above the desorption equilibrium pressures of MgH_2 and Mg_2FeH_6. Once the desorption pressure is below the respective equilibrium pressures of the hydride phases, the desorption process starts. Thus, in the first step MgH_2 decomposes. Then, a plateau period appears till the desorption equilibrium pressure of Mg_2FeH_6 is reached. Finally, in the second step, the Mg_2FeH_6 decomposition occurs.

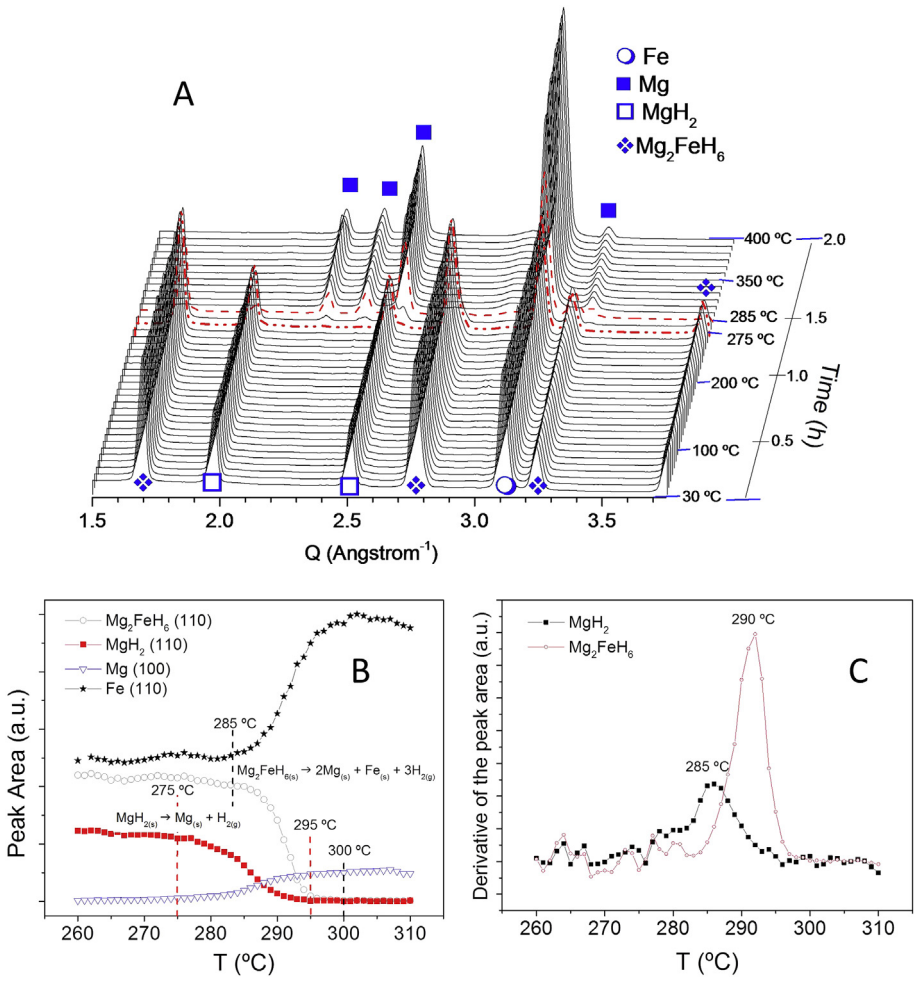

Fig. 5 – In-situ SR-PXD of a 2Mg–Fe stoichiometric mixture after the preparation process. A – Dehydriding from 30 to 400 °C and 0.1 MPa of H_2. B – Peak area of Mg (100), Fe (110), MgH_2 (110) and Mg_2FeH_6 (110) as a function of the temperature from 260 to 310 °C. C – Derivative as a function of the temperature for MgH_2 (110) and Mg_2FeH_6 (110). Heating rate ~3 °C/min.

At 300 °C, the desorption curves (Fig. 6B) just show a single step reaction which belongs to the MgH_2 decomposition. In Fig. 6D curve (5) at 350 °C, a two step desorption process can be seen. It suggests that the Mg_2FeH_6 is only formed at pressures above 4.4 MPa at 350 °C (isothermal conditions). At 400 °C, the MgH_2–Mg_2FeH_6 hydride mixture is even present at a pressure nearby the equilibrium one. These results are in agreement with the in-situ SR-PXD experiments (Figs. 2 and 5). At temperatures above 350 °C, the pressure enhances the formation of Mg_2FeH_6 (Fig. 6C, D, E and F). However, as observed during the sintering processes carried out at 400 °C and 6.0 MPa and 12.0 MPa, no difference was noticed in the MgH_2–Mg_2FeH_6 hydride mixture composition. Therefore, at isothermal conditions, the Mg_2FeH_6 formation is meanly enhanced by higher temperatures. It is important to mention that higher temperatures can also cause material disproportion due to the high vapor pressure of Mg, hence leading to the incomplete formation of Mg_2FeH_6 [2].

In order to analyze more in detail the temperature effect, additional measurements were done. In Fig. 7A, absorption measurements at 350, 375 and 400 °C performed at the same driving force of Pi/Peq. equal to 2.7 are shown. After absorption, the samples were characterized by PXD (Fig. 7B) and DSC (Fig. 7C). It can be noticed that the absorption reaction rates are slower as the temperature goes up (Fig. 7A). At 350 °C and low Pi/Peq. ratio in comparison with the Pi/Peq. of 5.1 at which Mg_2FeH_6 appears (Fig. 6C and D – curves (5)), MgH_2, Fe and Mg are only detected by PXD (Fig. 7B (c)). These low temperature and pressure conditions do not allow the formation of Mg_2FeH_6 since the effective solid–solid diffusion mechanisms are hindered (see Section 3.1.1). Thus, the absorption rate at 350 °C can be ascribed to the fast formation of MgH_2 catalyzed by Fe (Fig. 7A (c)). On the other hand, the PXD patterns of the samples hydrided at 375 and 400 °C show the presence of Mg_2FeH_6, MgH_2 and remnant Fe. Moreover, based on the PXD peak areas, the relative amount of Mg_2FeH_6 increases as the temperature rises from 375 to 400 °C. At these high temperature conditions, the above mentioned diffusion effects are overcome, allowing the Mg_2FeH_6 formation and leading to a slower kinetic behavior (Fig. 7A (b) and (a)) [5].

As seen in Fig. 7C, the decomposition DSC curves of the hydrided samples (Fig. 7A) are compared. The sample hydrided at 350 °C (Fig. 7C (c)) only exhibits an endothermic event corresponding to the MgH_2 decomposition (see PXD – Fig. 7B

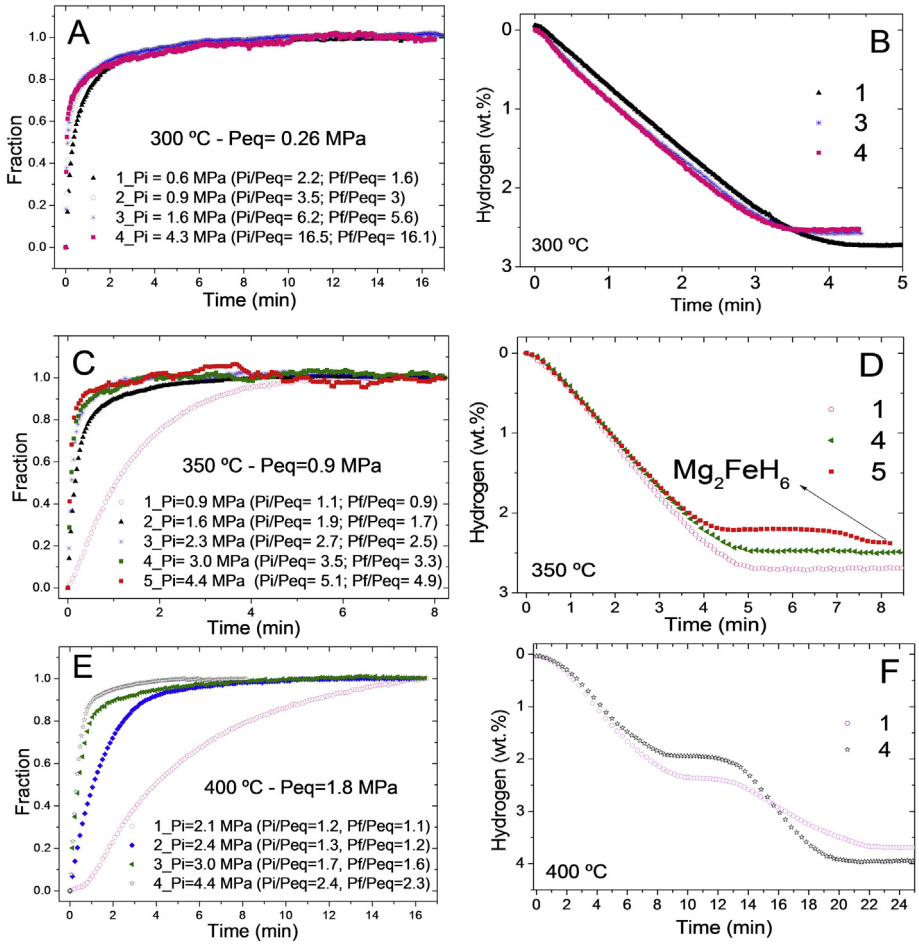

Fig. 6 – Hydrogen sorption curves of the Mg_2FeH_6–MgH_2 hydride mixture as a function of the pressure at 300, 350 and 400 °C: A – at 300 °C and from 0.6 to 4.3 MPa, C – at 350 °C in the range of pressure from 0.9 to 4.4 MPa, E – at 400 °C and from 2.1 to 4.4 MPa. B, D, F – at 300, 350 and 400 °C and from a pressure over the Peq. (Equilibrium pressure) to 20 kPa.

(c)). On the other hand, it can be observed that both samples hydrided at 375 and 400 °C show two endothermic events (Fig. 7C (b) and (a)).

According to the results shown in Section 3.1.2 – Dehydrogenation path of the Mg–Fe–H hydride system (Fig. 6D and F and Fig. 7B (a) and (b)), the first step of the dehydriding reaction of MgH_2–Mg_2FeH_6 belongs to the decomposition of MgH_2 and the second to the decomposition of Mg_2FeH_6. Furthermore, as seen in the DSC curves (Fig. 7C (a), (b) and (c)), the peak maxima of the first endothermic event (MgH_2) are between 275 and 280 °C which is in good correlation with the analysis shown in Fig. 5C. In the case of the second thermal event (Mg_2FeH_6), the peak areas increase with the temperature as the intensity of the PXD reflections of Mg_2FeH_6 (Fig. 7B (b) and (a)). The peak maxima of Mg_2FeH_6 decomposition are at 300 (Fig. 7C (b)) and 310 °C (Fig. 7C (a)), while the obtained in Fig. 5C is at 290 °C. Additionally, the material composed of Mg_2FeH_6 plus remnant Fe has a peak maximum at 310 °C (Fig. 4B (e)) which is in agreement with the thermal events associated with Mg_2FeH_6 decomposition in Fig. 7C. Other important characteristics are: (1) the broadening of the DSC peaks as the material contains the MgH_2–Mg_2FeH_6 hydride mixture, (2) lower starting temperature of hydrogen release at about 210 °C (Fig. 7C (b) and (a)) in comparison with 250 °C for MgH_2 (Fig. 7C (c)) and (3) the lower temperatures of the peak maxima of Mg_2FeH_6 as the amount of MgH_2 increases. These characteristics can be related to a broader particle size distribution and to a better microstructural refinement along with the interaction between MgH_2 and Mg_2FeH_6 [15–17]. This issue will be addressed more in detail in the following section.

3.2.2. *Desorption kinetics: activation energy*

In order to investigate the decomposition behavior of the MgH_2–Mg_2FeH_6 hydride mixture, the desorption activation energies (E_a) for samples hydrided at different conditions were calculated. Additionally, these samples were characterized by PXD and DSC. To obtain materials with similar microstructural characteristics, all samples were prepared from the same starting material and basic procedure. As starting material, 2Mg–Fe stoichiometric mixture milled 100 h in Ar plus sintering at 400 °C and 6.0 MPa of H_2 was used. This material was then subjected to a non-isothermal dehydriding (10 °C/min) till 400 °C and at 20 kPa. Three samples were prepared with the obtained 2Mg–Fe dehydrogenated material: (1) sample hydrided at 300 °C and 3.7 MPa of H_2, (2) sample hydrided at 400 °C and 2.2 MPa of H_2 and (3) sample hydrided

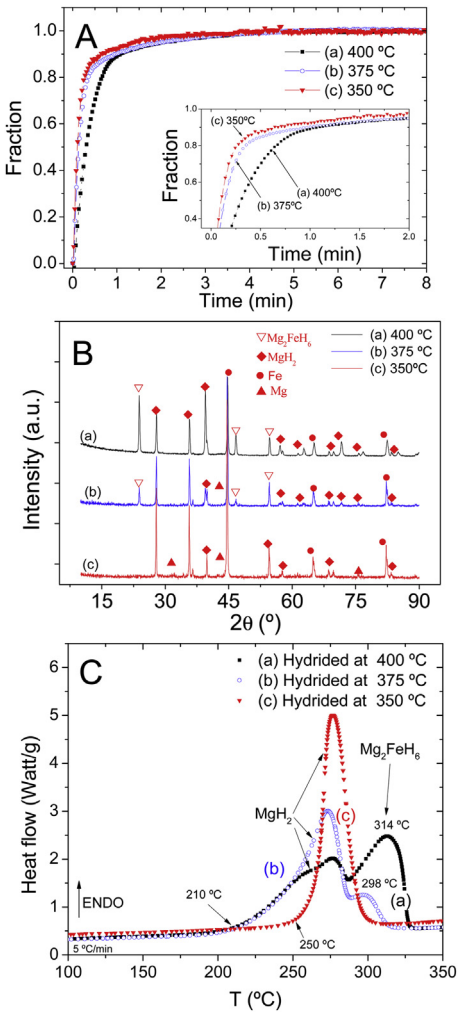

Fig. 7 – A – Hydrogen absorption curves of the Mg_2FeH_6–MgH_2 hydride mixture obtained from a milled and sintered 2Mg–Fe stoichiometric mixture: (c) 350, (b) 375 and (a) 400 °C using a relationship of Pi/Peq. equal to 2.7. B – Lab. PXD and C – DSC (5 °C min^{-1}) of the hydrided samples at (c) 350, (b) 375 and (a) 400 °C.

at 400 °C and 2.2 MPa of H_2 and then dehydrided at 300 °C and 20 kPa down to 2 wt.% H. These procedures were performed in the Sieverts kind device [38].

In Fig. 8 the DSC curves (Fig. 8A) and PXD (Fig. 8B) of the as described above prepared samples are shown. The sample (1) hydrided at 300 °C just exhibits an endothermic event (Fig. 8A (a)) owing to the decomposition of MgH_2 (PXD – Fig. 8B (a)). On the other hand, the samples (2) hydrided at 400 °C (Fig. 8A (b)) and (3) hydrided at 400 °C – dehydrided at 300 °C down to 2 wt.% H (Fig. 8A (c)), show two endothermic processes corresponding to MgH_2 and Mg_2FeH_6 (PXD – Fig. 8B (b) and (c)). Taking into account that the decomposition of MgH_2 first starts (see Fig. 5 – Section 3.1.2 and Fig. 6 – Section 3.2.1), the sample dehydrided down to 2 wt.% H just has a small amount of MgH_2, being Mg_2FeH_6 the hydride phase in the higher proportion. The observed decomposition behavior (Fig. 8A) is in agreement with the results obtained by in-situ SR-PXD (Fig. 5) and with those shown in Fig. 7B and C. In Table 1, the preparation conditions and the major hydride phases (underlined) in (1), (2) and (3) samples are indicated.

In Fig. 9 the Kissinger plots for the activation energies (E_a) of the dehydrided processes of the above described samples (1), (2) and (3) (Fig. 8A and B) are shown. As comparison, the sample composed of Mg_2FeH_6 and remnant Fe described in Section 3.1.1 – Fig. 4A(e) and B(e) is also included. As seen, two regions belonging to MgH_2 and Mg_2FeH_6 are distinguished (separated by a green dashed line). In Table 1, a comparison between the decomposition E_a values obtained here and those reported in the literature is presented.

Previous works [12,15] showed that there is no clear correlation between the decomposition E_a and the microstructural characteristics of the material. Moreover, it was found that a MgH_2–Mg_2FeH_6 hydride mixture synthesized by milling in H_2 atmosphere decomposes in a single endothermic process. This fact was attributed to the small and well crystallized hydride particles [15]. In our case, it is possible to differentiate two endothermic events and to calculate the decomposition E_a for both (Fig. 8A (b) and (c); Fig. 9 (b) and (c)). It can be noticed that the E_a of the second thermal event (Fig. 8A) associated with the Mg_2FeH_6 decomposition decreases as the amount of MgH_2 in the hydride mixture increases (see Table 1). In the literature [11,12,15], the decomposition E_a values of Mg_2FeH_6 without MgH_2 are much higher. This fact is related to the oxidation (MgO) in some cases and in others to the preparation process (Table 1). The oxidation on the surface of the material can hinder the recombination of hydrogen molecule, while a low degree of microstructural refinement can delay the hydrogen release. Thus, both effects can increase the decomposition E_a. In some cases, though, oxidation is not detected and the material is synthesized by milling in hydrogen atmosphere, which would lead to lower decomposition E_a. However, for a material composed of Mg_2FeH_6 + Fe synthesized by 270 h of milling in H_2, the decomposition E_a value is rather high (257.6 ± 9.1 kJ/mol H_2) [15].

In the case of MgH_2, the calculated E_a values (Fig. 9(a), (b) and (c)) are higher than that reported for MgH_2 catalyzed by Fe (see Table 1) [11]. For the samples hydrided at 300 °C (Fig. 9(a)) and 400 °C (Fig. 9(b)) the E_a values are nearby the value of as-milled MgH_2 (see Table 1) [11] which can be related to the microstructural characteristics conferred by the synthesis, i.e. milling + sintering or milling in H_2 [45]. The E_a values for MgH_2 decomposition might follow a trend for the samples hydrided at 300 °C (Fig. 9(a), 167 ± 3 kJ/mol H_2) and at 400 °C (Fig. 9(b), 151 ± 7 kJ/mol H_2). However, the sample desorbed down to 2 wt.% H presents an unusual high value (Fig. 9(c), 330 ± 30 kJ/mol H_2) with a large error band. It can be ascribed to the small quantity of MgH_2 in the sample that did not allow the determination of more than 3 points, with high uncertainty degree. Despite this, the presence of Mg_2FeH_6 also seems to influence the MgH_2 decomposition.

Zaluska et al. [48] investigated the decomposition behavior of as-milled Mg_2NiH_4–MgH_2 mixtures. It was found that the presence of Mg_2NiH_4 and MgH_2 results in a synergetic effect enhancing the decomposition properties. This fact was attributed to the interaction between Mg_2NiH_4 and MgH_2 through contraction – strain mechanisms upon dehydriding. Besides, the decomposition temperature of pure

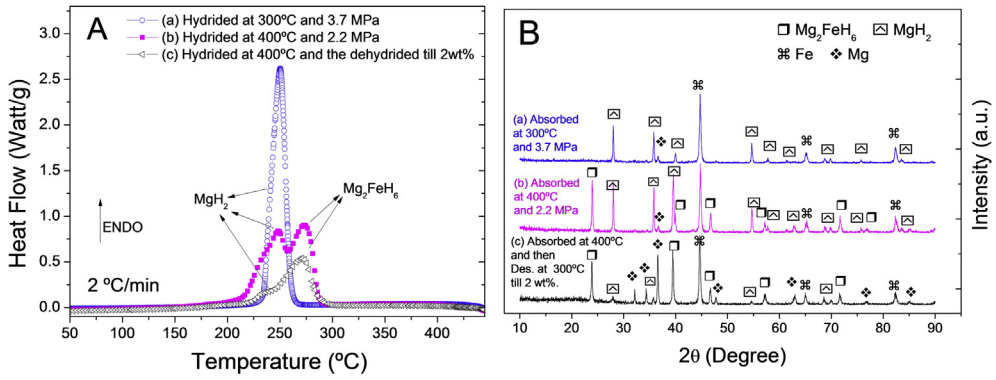

Fig. 8 – Characterization by A – DSC (2 °C min^{-1}) and B – Lab. PXD of the 2Mg–Fe stoichiometric mixture after the synthesis at different conditions: (a) sample hydrided at 300 °C and 3.7 MPa (absorbed hydrogen capacity: 2.9 wt.% H), (b) sample hydrided at 400 °C and 2.2 MPa (absorbed hydrogen capacity: 3.7 wt.% H), (c) sample hydrided at 400 °C and 2.2 MPa (absorbed hydrogen capacity: 4 wt.%) and then dehydrided at 300 °C till 2 wt.% H.

Mg_2NiH_4 is lower than that corresponding to MgH_2, thus Mg_2NiH_4 decomposition acted as trigger for the MgH_2 dehydriding.

In the case of MgH_2–Mg_2FeH_6 hydride mixture, the MgH_2 decomposes before Mg_2FeH_6. However, the starting decomposition temperature of MgH_2 in the mixture (Fig. 7C (a) and (b); Fig. 8A(b)) is being lowered. Moreover, there exists a correlation between the temperature of the peak maxima and the decomposition E_a of Mg_2FeH_6 with the relative amount of MgH_2 in the mixture ((Fig. 7C (a) and (b); Fig. 9; Table 1). Both, peak maxima and the decomposition E_a of Mg_2FeH_6 are lowered as the MgH_2 quantity increases. Thus, the former MgH_2 decomposition can activate the latter Mg_2FeH_6 decomposition lowering the temperature of the peak maxima and acting as a destabilizing agent in terms of E_a.

It is possible to conclude that the enhanced decomposition behavior of the MgH_2–Mg_2FeH_6 hydride mixture might be ascribed to a dual synergetic-destabilizing effect of both hydrides on each other. On one hand, the presence of both hydrides results in a material with improved microstructural characteristics leading to a mutual interaction during dehydriding, i.e. contraction – strain mechanisms acting as decomposition activators. On the other hand, destabilizing effects can lower the decomposition E_a, meanly for Mg_2FeH_6.

3.3. *Phase diagram of the Mg–Fe–H hydride system*

The study of the thermodynamic [4,5] and kinetic (Figs. 5 and 6) behaviors of the Mg–Fe–H hydride system allows to build a phase diagram. Fig. 10 describes the temperature and pressure

Table 1 – Decomposition activation energy: Comparison between the values obtained in this work and those reported in the literature [11,12,15]. In the first three lines, underlined compounds (MgH_2 and Mg_2FeH_6) correspond to major hydride phases in the material (based on PXD peak intensities).

Staring material	Preparation method	Detected phases (PXD)	E_a (kJ/mol H_2)	Ref.
2Mg–Fe	(1) – 100 h MM in Ar + Sintering, then des. Non-isothermal till 400 °C and rehydriding at 300 °C and 3.7 MPa –Fig. 9 – (c)	$\underline{MgH_2}$, Mg and Fe	167 ± 3	This work
2Mg–Fe	(2) – 100 h MM in Ar + Sintering, then des. Non-isothermal till 400 °C and rehydriding at 400 °C and 2.2 MPa –Fig. 9 – (a)	$\underline{MgH_2}$, $\underline{Mg_2FeH_6}$, Mg and Fe	Peak 1: 151 ± 7 Peak 2: 104 ± 2	This work
2Mg–Fe	(3) – 100 h MM in Ar + Sintering, then des. Non-isothermal till 400 °C, then rehydriding at 400 °C and 2.2 MPa and finally desorption at 300 °C till 2 wt.% H – Fig. 9 – (b)	MgH_2, $\underline{Mg_2FeH_6}$, Mg and Fe	Peak 1: 330 ± 30 Peak 2: 113 ± 7	This work
$2MgH_2$–Fe	Repeated four times: Milled 2 h and sintered at 450 °C and 6.0 MPa (Fig. 4B – curve (e))	Mg_2FeH_6 and Fe	132 ± 9	This work
MgH_2	Milled 30 h	MgH_2	168 ± 36	[11]
2Mg–Fe	Milled 30 h in H_2 atmosphere	MgH_2 and Fe	110 ± 10	[11]
2Mg–Fe	Milled 60 h in H_2 atmosphere	Mg_2FeH_6, MgO and Fe	174 ± 36	[11]
2Mg–Fe	Fe pre-milled 100 h in H_2 atmosphere, then 2Mg + pre-milled Fe milled 210 h in H_2 atmosphere	Mg_2FeH_6, MgO and Fe	162 ± 2	[12]
2Mg–Fe	Milled 270 h in H_2 atmosphere (with sample substraction)	Mg_2FeH_6, MgO and Fe	185 ± 3	[12]
2Mg–Fe	Milled 270 h in H_2 atmosphere (without sample substraction)	Mg_2FeH_6 and Fe	257.6 ± 9.1	[15]

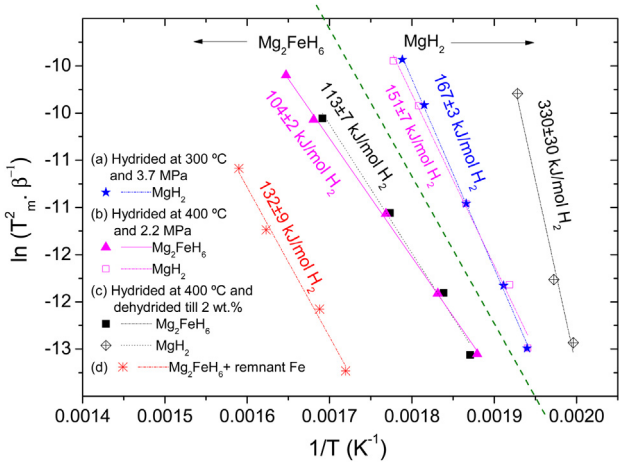

Fig. 9 – Decomposition activation energy: Kissinger plots of the 2Mg–Fe stoichiometric mixture after the synthesis and hydrided – dehydrided processes at different conditions: (a) sample hydrided at 300 °C and 3.7 MPa, (b) sample hydrided at 400 °C and 2.2 MPa, (c) sample hydrided at 400 °C and 2.2 MPa and then dehydrided at 300 °C till 2 wt.% H, (d) $2MgH_2$–Fe after four consecutive thermal processes (composed of: Mg_2FeH_6 and Fe, from Section 3.1.1 – Fig. 4A(e) and B(e)).

conditions at which the Mg_2FeH_6–MgH_2 hydride mixture is obtained. The absorption equilibrium conditions for the Mg_2FeH_6–MgH_2 are drawn in black curve with circle points. Both desorption equilibrium conditions for MgH_2 and Mg_2FeH_6 are shown in dash blue curve with square points and point green curve with triangle points, respectively. Under dynamic conditions (indicated by black stars), at temperatures ≤350 °C and pressures ≤4.4 MPa, the Mg–Fe–H hydride system is only composed of MgH_2 + Fe and remnant Mg, while at higher temperatures and pressures $Mg2FeH_6 + MgH_2$ and remnant Fe are present (magenta rhombic points).

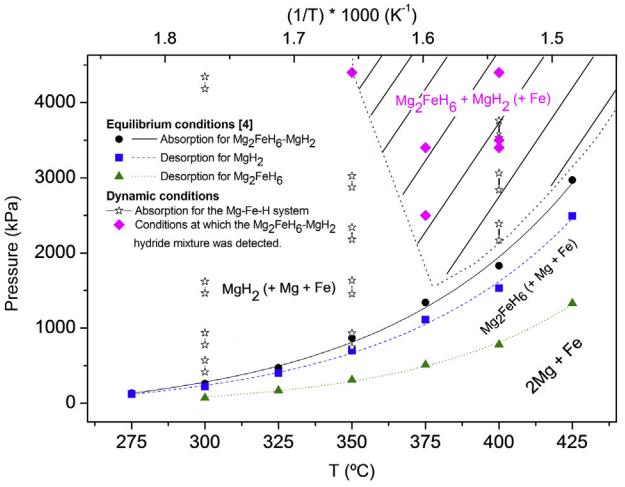

Fig. 10 – Phase diagram of the Mg–Fe–H system obtained from as-milled and hydrided 2Mg–Fe stoichiometric sample. ● — Absorption equilibrium pressures of the Mg_2FeH_6–MgH_2 hydride mixture, ▪ - Desorption equilibrium pressures of MgH_2, ▲. Desorption equilibrium pressures of Mg_2FeH_6. Dynamic conditions: –✶ – Absorption temperature and pressures (initial and final pressure of the absorption process shown in Fig. 5). ◆ Pressure and temperature conditions at which the Mg_2FeH_6–MgH_2 hydride mixture is obtained.

4. Conclusions

Based on our results, the Mg_2FeH_6 formation comprises a two-steps reaction with MgH_2 as an intermediate phase. Moreover, the reaction during the hydrogen absorption process is hindered by slow solid–solid diffusion, thus leading to the MgH_2–Mg_2FeH_6 hydride mixture formation. The dehydrogenation process of the obtained MgH_2–Mg_2FeH_6 hydride mixture follows two almost simultaneous and independent reactions. First, MgH_2 decomposes into Mg. Then Mg_2FeH_6 desorbs hydrogen giving directly elemental Mg and Fe as products. Moreover, the observed desorption behavior and calculated decomposition activation energy values indicate that the Mg_2FeH_6–MgH_2 hydride mixture decomposes via synergetic-destabilizing effects as a result of hydride phases interactions. An analysis of the pressure and temperature effects upon the kinetic characteristics of MgH_2–Mg_2FeH_6 hydride mixture showed that at temperatures ≤350 °C and pressures ≤4.4 MPa, the Mg–Fe–H hydride system is only composed of MgH_2 + Fe and remnant Mg, while above 350 °C and 4.4 MPa the hydride phases Mg_2FeH_6 and MgH_2 plus remnant Fe are present.

Acknowledgments

The authors thank CONICET (Consejo Nacional de Invetigaciones Científicas y Técnicas), DAAD (German Academic Exchange Service) – Ministerio de Educación de la Nación Argentina (Sandwich Grant Program), ANPCyT (Agencia Nacional de Promoción Científica y Tecnológica), CNEA (Comisión Nacional de Energía Atómica) and Instituto Balseiro (UNCuyo) for financial support to carry out this work.

REFERENCES

[1] Didisheim J-J, Zolliker P, Yvon K, Fischer P, Schefer J, Gubelmann M, et al. Dimagnesium iron (II) hydride, Mg_2FeH_6, containing octahedral FeH_6^{4-} anions. Inorg Chem 1984;23:1953–7.

[2] Bodanović B, Reiser A, Schlichte K, Spliethoff B, Tesche B. Thermodynamics and dynamics of the Mg–Fe–H system and its potential for thermochemical thermal energy storage. J Alloys Compd 2002;345:77–89.

[3] Konstanchuk YG, Ivanov E, Pezat M, Darriet B, Boldyrev V, Hagenmuller P. The hydriding properties of a mechanical alloy with composition Mg-25%Fe. J Less-Common Met 1987;131:181–9.

[4] Puszkiel JA, Arneodo Larochette P, Gennari FC. Thermodynamic and kinetic studies of Mg–Fe–H after mechanical milling followed by sintering. J Alloys Compd 2008;463:134–42.

[5] Puszkiel JA, Arneodo Larochette P, Gennari FC. Thermodynamic–kinetic characterization of the synthesized

Mg_2FeH_6–MgH_2 hydrides mixture. Int J Hydrogen Energy 2008;33:3555–60.
[6] Massalski T, editor. Binary alloy phase diagrams. 2nd ed. Metals Park, OH: American Society for Metals; 1990.
[7] Selvam P, Yvon K. Synthesis of Mg_2FeH_6, Mg_2CoH_5 and Mg_2NiH_4. Int J Hydrogen Energy 1991;16(9):615–7.
[8] Bodanovič B, Reiser A, Schlichte K, Seastre TO, editors. Hydrogen power: theoretical and engineering solutions. Kluwer Academic Publisher; 1998. p. 291–6.
[9] Reiser A, Bodanovič B, Schlichte K. The application of Mg-based metal–hydrides as heat energy storage system. Int J Hydrogen Energy 2000;25:425–30.
[10] Huot J, Boily S, Akiba E, Schulz R. Direct synthesis of Mg_2FeH_6 by mechanical alloying. J Alloys Compd 1998;280:306–9.
[11] Gennari F, Castro F, Andrade Gamboa JJ. Synthesis of Mg_2FeH_6 by reactive mechanical alloying: formation and decomposition properties. J Alloys Compd 2002;339:261–7.
[12] Song-lin L, Varin RA, Morozova O, Khomenko T. Controlled mechano-chemical synthesis of nanostructured ternary complex hydride Mg_2FeH_6 under low-energy impact mode with and without pre-milling. J Alloys Compd 2004;384:231–48.
[13] Varin RA, Li S, Calka A, Wexler D. Formation and environmental stability of nanocrystalline and amorphous hydrides in the 2Mg–Fe mixture processed by controlled reactive mechanical alloying (CRMA). J Alloys Compd 2004;373:270–86.
[14] Castro F, Gennari FC. Effect of the nature of the starting materials on the formation of Mg_2FeH_6. J Alloys Compd 2004;375:292–6.
[15] Varin RA, Li S, Wronski Z, Morozova O, Khomenko T. The effect of sequential and continuous high-energy impact mode on the mechano-chemical synthesis of nanostructured complex hydride Mg_2FeH_6. J Alloys Compd 2005;390:282–96.
[16] Varin RA, Li S, Chiu Ch, Guo L, Morozova O, Khomenko T, et al. Nanocrystalline and non-crystalline hydrides synthesized by controlled reactive mechanical alloying/milling of Mg and Mg–X (X = Fe, Co, Mn, B) systems. J Alloys Compd 2005;404–406:494–8.
[17] Zhou DW, Li SL, Varin RA, Peng P, Liu JS, Yang F. Mechanical alloying and electronic simulations of 2Mg–Fe mixture powders for hydrogen storage. Mater Sci Eng A 2006;427:306–15.
[18] Wronski Z, Varin RA, Chiu C, Czujko T, Calka A. Mechanochemical synthesis of nanostructured chemical hydrides in hydrogen alloying mills. J Alloys Compd 2007;434–435:743–6.
[19] Song-lin L, Sheng-long T, Yi L, Shu-ke P, Jian-min C. Synthesis of nanostructured Mg_2FeH_6 hydride and hydrogen sorption properties of complex. Trans Nonferrous Met Soc China 2010;20:2281–8.
[20] Lima GF, Peres MM, Garroni S, Baró MD, Surinyach S, Kiminami CS, et al. Microstructural characterization and hydrogenation study of extruded MgFe alloy. J Alloys Compd 2010;504S:S299–301.
[21] Asselli AAC, Jorge Jr AM, Ishikawa TT, Botta WJ. Mg_2FeH_6-based nanocomposites with high capacity of hydrogen storage processed by reactive milling. Mater Res 2012;15(2):229–35.
[22] Asselli AAC, Leiva DR, Jorge Jr AM, Ishikawa TT, Botta WJ. Synthesis and hydrogen sorption properties of MgH_2–Mg_2FeH_6 nanocomposites prepared by reactive milling. J Alloys Compd 2012;5365:S250–4.
[23] Polanski M, Katarzyna W, Nielsen TK, Jaroszewicz L, Bystrzycki J. The influence of the milling time on the yield of Mg_2FeH_6 from a two-step synthesis conducted in a custom-made reactor. Int J Hydrogen Energy 2013;38:2785–9.
[24] Ivanov E, Konstanchuk I, Stepanov A, Boldyrev V. Magnesium mechanical alloys for hydrogen storage. J Less-Common Met 1987;131:25–9.
[25] Huot J, Hayakawa H, Akiba E. Preparation of the hydrides Mg_2FeH_6 and Mg_2CoH_5 by mechanical allying followed by sintering. J Alloys Compd 1997;248:164–7.
[26] Riktor MD, Deledda S, Herrich M, Gutfleisch O, Fjellvåg H, Hauback BC. Hydride formation in ball-milled and cryomilled Mg–Fe powder mixtures. Mater Sci Eng B 2009;158:19–25.
[27] Polanski M, Nielsen TK, Cerenius Y, Bystrzycki J, Jensen TR. Synthesis and decomposition mechanisms of Mg_2FeH_6 studied by in-situ synchrotron X-ray diffraction and high-pressure DSC. Int J Hydrogen Energy 2010;35:3578–82.
[28] Zhang J, Cuevas F, Zaïdi W, Bonnet J-P, Aymard L, Bobet J-L, et al. Highlighting of a single reaction path during reactive ball milling of Mg and TM by quantitative H_2 gas sorption analysis to form ternary complex hydrides (TM = Fe, Co, Ni). J Phys Chem C 2011;115(11):4971–9.
[29] Bläsius A, Gonser U. Mössbauer surface studies on TiFe hydrogen storage material. Appl Phys 1980;22:331–2.
[30] Welter J-M, Rudman PS. Iron catalyzed hydriding of magnesium. Scripta Metall 1982;16:285–6.
[31] Liang G, Huot J, Boily S, Van Neste A, Schulz R. Caralytic effect of transition metals on hydrogen sorption in nanocrystalline ball milled MgH_2–Tm (Tm = Ti, V, Mn, Fe and Ni) systems. J Alloys Compd 1999;292:247–52.
[32] Hanada N, Ichikawa T, Fujii H. Catalytic effect of nanoparticle 3d-transition metals on hydrogen storage properties in magnesium hydride MgH_2 prepared by mechanical milling. J Phys Chem B 2005;109:7188–94.
[33] Bobet J-L, Akiba E, Nakamura Y, Darriet B. Study of Mg-M (M = Co, Ni, Fe) mixture elaborated by reactive mechanical alloying – hydrogen sorption properties. Int J Hydrogen Energy 2000;25:987–96.
[34] Berlouis LEA, Cabrera E, Hall-Barientos E, Hall PJ, Dodd SB, Morris S, et al. Thermal analysis investigation of hydriding properties of nanocrystalline MgeNi and MgeFe-based alloys prepared by high-energy ball milling. J Mater Res 2001;16:45–57.
[35] Bassetti A, Bonetti E, Pasquini L, Montone A, Grbovic J, Vittori Antisari M. Hydrogen desorption from ball milled MgH_2 catalyzed with Fe. Eur Phys J B 2005;43:19–27.
[36] Cerenius Y, Staal K, Svensson LA, Usby T, Oskasson A, Albertson J, et al. The crystallography beamline I711 at MAX II. Synchrotron Rad 2000;7:1–399.
[37] Jensen TR, Nielsen TK, Filinchuk Y, Jørgensen JE, Cerenius Y, Gray EM, et al. Versatile in-situ powder X-ray diffraction cells for solid-gas investigations. J Appl Cryst 2010;43(6):1456–63.
[38] Meyer G, Rodríguez DS, Castro F, Fernández G. Automatic device for precise characterization of hydride forming materials. In: Hydrogen energy progress, proceedings of the 11th world energy conference, Stuttgart, Germany 23–29 Junio 1996. p. 1293–8.
[39] Schulz R, Huot J, Boily S. Can. Patent, Ser. – Nr. 2207149; 1999.
[40] Alexander L, Klug PH. Determination of crystallite size with the X-ray spectrometer. J Appl Phys 1950;21:137–42.
[41] Kissinger HE. Reaction kinetics in differential thermal analysis. Anal Chem 1957;29:1702–6.
[42] Khawam A, Flanagan DR. Solid-state kinetic models: basics and mathematical fundamentals. J Phys Chem B 2006;110:17315–28.
[43] Stampfer Jr JF, Holley Jr CE, Suttle JF. The magnesium-hydrogen system. J Am Chem Soc 1959;82:3504–8.
[44] Bodanovič B, Bohmhammel K, Christ B, Reiser A, Schlichte K, Vehlen R, et al. Thermodynamic investigation of the

magnesium–hydrogen system. J Alloys Compd 1999;282:84–92.
[45] Čermák J, Král L. Hydrogen diffusion in Mg–H and Mg–Ni–H alloys. Acta Mater 2008;56:2677–86.
[46] Zaluska A, Zaluski L, Ström-Olsen JO. Nanocrystalline magnesium for hydrogen storage. J Alloys Compd 1999;288:217–25.
[47] Herrich M, Ismail N, Lyubina J, Handstein A, Pratt A, Gutfleisch O. Synthesis and decomposition of Mg_2FeH_6 prepared by reactive milling. Mater Sci Eng B 2004;108:28–32.
[48] Zaluska A, Zaluski L, Ström-Olsen JO. Synergy of hydrogen sorption in ball-milled hydrides of Mg and Mg_2Ni. J Alloys Compd 1999;289:197–206.